Downloaded from orbit.dtu.dk on: May 10, 2024

DTU Library

Experimental investigation on dry electrical discharge machining using helium gas

Puthumana, Govindan; Agarwal, Rahul; S. Joshi, Suhas

Published in:
Proceedings of the 3rd International & 24th AIMTDR

Publication date:
2010

Document Version
Peer reviewed version

Link back to DTU Orbit

Citation (APA):
Puthumana, G., Agarwal, R., & S. Joshi, S. (2010). Experimental investigation on dry electrical discharge machining using helium gas. In *Proceedings of the 3rd International & 24th AIMTDR*

General rights
Copyright and moral rights for the publications made accessible in the public portal are retained by the authors and/or other copyright owners and it is a condition of accessing publications that users recognise and abide by the legal requirements associated with these rights.

- Users may download and print one copy of any publication from the public portal for the purpose of private study or research.
- You may not further distribute the material or use it for any profit-making activity or commercial gain
- You may freely distribute the URL identifying the publication in the public portal

If you believe that this document breaches copyright please contact us providing details, and we will remove access to the work immediately and investigate your claim.

3rd International & 24th AIMTDR (All India Manufacturing Technology, Design and Research),

A.U. College of Engineering (A), Andhra University, Visakhapatnam, December 13-15, 2010.

Experimental investigation on dry electrical discharge machining using helium gas

[1]Govindan P., [2]Rahul Agarwal., [3]Suhas S Joshi.

[1]Ph.D candidate,Department of Mechanical Engineering, I I T Bombay, India.

E-mail: govindan@iitb.ac.in

[2]B Tech student,Department of Mechanical Engineering, I I T Bombay, India.

E-mail: rahulagrawal@iitb.ac.in

[3]Professor, Department of Mechanical Engineering, I I T Bombay, India.

E-mail: ssjoshi@iitb.ac.in

Abstract:- In a dry EDM process, a gaseous dielectric replaces the liquid dielectric. Low MRR, arcing and damage on machined surfaces are the critical issues of this process. This work aims to examine the viability of dry EDM using helium gas dielectric. Experiments were performed to explore the effects of parameters such as voltage (*V*), current (*I*), pulse 'off-time' (T_{off}), gas pressure (*P*) and spindle speed (*N*) on MRR, TWR, oversize and depth achieved. Statistical analysis using ANOVA showed that spindle speed (*N*) and discharge current (*I*) were the most significant in influencing the MRR and the oversize respectively. Analysis of dry EDMed surface morphology indicated that surface damages were lesser by using helium than using oxygen gas dielectric.

Keywords: *Dry EDM, helium, MRR, TWR, oversize, depth.*

1. INTRODUCTION

Dry electrical discharge machining is an environment friendly EDM technique in which gas at high pressure is used as the dielectric medium instead of mineral oil-based liquid dielectric. Dry EDM has a few advantages such as near-zero tool electrode wear [1,2], simpler machine configurations [1], formation of a thinner recast layer [3,4], lower thermal damage of machined surface [5-10] and low viscosity of gaseous dielectric helping debris flushing from the inter-electrode gap [6]. Recently, a study has been done by the authors' research group to investigate dry EDM using oxygen gas by employing an aluminium shield around the plasma to restrict unlimited expansion of the plasma [10].

In the present work, an investigation on dry EDM process using helium gas dielectric has been done. An aluminium shield has been employed around the dry EDM plasma to create a back pressure, to restrict the spreading out of the plasma. Effect of the input parameters, viz. gap voltage (*V*), discharge current (*I*), pulse-off time (T_{off}), gas pressure (*P*), spindle speed (*N*) and shield clearance at bottom (C_b) on material removal rate (MRR), tool wear rate (TWR), oversize and depth has been studied using Taguchi L_8 orthogonal array. Also, the quality of the machined surfaces has been analysed using scanning electron microscopy (SEM).

2. EXPERIMENTAL WORK

2.1 Experimental design

In this experimentation, various independent parameters were selected based on the preliminary experiments and past literature on dry EDM. Experiments were done using L_8 orthogonal array. The levels of input parameters, allotment of parameters to the array and response variables are presented in Table 1.

Table 1. L_8 array with levels of input parameters, their allocation and response variables

Expt No.	V (volts)	I (A)	C_3	T_{off} (μs)	P (MPa)	N (rpm)	C_b (mm)	Original trials				1st replication			
								MRR (mm^3/min)	TWR (mm^3/min)	Over size (%)	Depth (mm)	MRR (mm^3/min)	TWR (mm^3/min)	Over size (%)	Depth (mm)
1.	50	12	1	22	0.15	100	4	0.0096	0.0056	-1.45	0.12	0.0096	0.0309	2.17	0.13
2.	50	12	1	67	0.25	300	5	0.0160	0.0084	1.57	0.14	0.0256	0.0112	-2.50	0.38
3.	50	18	2	22	0.15	300	5	0.0385	0.0197	-3.49	0.23	0.0417	0.0197	-5.78	0.29
4.	50	18	2	67	0.25	100	4	0.0128	0.0000	-17.1	0.14	0.0128	0.0000	0.98	0.13
5.	80	12	2	22	0.25	100	5	0.0064	0.0000	-0.38	0.21	0.0128	0.0000	1.10	0.16
6.	80	12	2	67	0.15	300	4	0.0224	0.0253	0.33	0.14	0.0192	0.0056	-12.1	0.21
7.	80	18	1	22	0.25	300	4	0.0160	0.0197	-5.72	0.25	0.0353	0.0056	-3.88	0.25
8.	80	18	1	67	0.15	100	5	0.0128	0.0449	-0.53	0.17	0.0128	0.0000	-1.86	0.15

MRR, TWR, oversize and depth achieved have been included as the response variables and are defined as follows:

$$\text{MRR } (mm^3/\text{min}) = \frac{\text{Weight loss (gms)}}{\rho_{ss}} \times \frac{1}{T_m} \times 1000 \quad \ldots\ldots (1)$$

where, ρ_{ss} is the density of the SS304 workpiece in g/cm^3 and T_m is the machining time in minutes.

$$\text{TWR } (mm^3/\text{min}) = \frac{\text{Weight loss (gms)}}{\rho_{cu}} \times \frac{1}{T_m} \times 1000 \quad \ldots\ldots (2)$$

where, ρ_{cu} is the density of the copper tool electrode in g/cm^3 and T_m is the machining time in minutes.

$$\text{Oversize(\%)} = \frac{((\text{OD}) \text{ electrode} - (\text{OD}) \text{ drilled hole})}{\text{Outside diameter of tool electrode}} \times 100 \quad \ldots\ldots (3)$$

2.2 Experimental set-up

The dry EDM experiments were conducted on a S50 CNC EDM machine. A rotary spindle with through spindle flushing capability was used to hold the pipe electrodes. A helium gas cylinder with a regulator for flow control was connected to the spindle.

The workpieces of SS304 material used were in the form of split specimens each of dimensions 27 mm × 14 mm × 10 mm. Tool electrodes of copper were in the form of pipes and were of dimensions (OD: 4.75 mm and ID: 3.25 mm) and length of each pipe was 60 mm.

Hollow cylindrical aluminium shields having a total height of 15 mm, with two different radial clearances (at two levels of 4 and 5 mm) around the electrode, near the sparking zone, were used [10]. Fig. 1 *a-b* shows the schematic representation and photograph of the setup, respectively.

2.3 Experimental procedure

The dry electrical discharge drilling experiments were performed in a random order. Two replications were performed after completing first set of experiments. In first replication, all the experiments were performed. In second replication, only 4 experiments (Exp. No. 3, 6, 7 and 8) were performed. Each experiment was continued for 40 minutes.The weight loss of workpiece and tool, during the dry EDM process, was measured using Sartorius CP 4235 precision scale. Knowing the density of stainless steel 304 (workpiece) and copper (electrode), MRR and TWR were estimated.

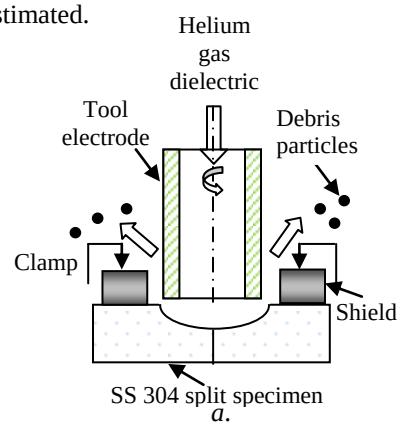

a.

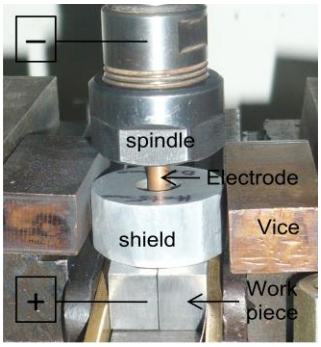

b.

Fig. 1 *a-b* Dry EDM using Helium gas dielectric a. Schematic representation *b*. Photograph of the experimental setup

Table 2 *a-d* ANOVA for a. MRR, b. TWR, c. Oversize, d. depth achieved

a. ANOVA for material removal rate (MRR)

Source	DF	Seq SS	Adj SS	Adj MS	F	P	Sig.
V	1	0.00009	0.00005	0.00005	1.12	0.310	×
I	1	0.00027	0.00024	0.00024	5.96	0.031	√
T_{off}	1	0.00024	0.00014	0.00014	3.56	0.083	×
P	1	0.00001	0.00000	0.00000	0.05	0.822	×
N	1	0.00125	0.00121	0.00121	30.0	0.000	√
C_b	1	0.00001	0.00001	0.00001	0.26	0.622	×
V×*I*	1	0.00002	0.00002	0.00002	0.61	0.449	×
Error	12	0.00048	0.00048	0.00004			
Total	19	0.00237					

b. ANOVA for tool wear rate (TWR)

Source	DF	Seq SS	Adj SS	Adj MS	F	P	Sig.
V	1	0.00002	0.00001	0.00001	0.03	0.858	×
I	1	0.00004	0.00003	0.00003	0.16	0.694	×
T_{off}	1	0.00004	0.00002	0.00002	0.09	0.774	×
P	1	0.00083	0.00088	0.00088	4.52	0.055	√
N	1	0.00012	0.00013	0.00013	0.65	0.436	×
C_b	1	0.00002	0.00002	0.00002	0.09	0.774	×
V×*I*	1	0.00008	0.00008	0.00008	0.39	0.545	×
Error	12	0.00235	0.00235	0.00020			
Total	19	0.00347					

c. ANOVA for oversize

Source	DF	Seq SS	Adj SS	Adj MS	F	P	Sig.
V	1	9.32	8.74	8.74	0.45	0.503	×
I	1	354.61	501.21	501.21	25.9	0.000	√
T_{off}	1	18.61	34.18	34.18	1.77	0.187	×
P	1	0.04	0.01	0.01	0.00	0.984	×
N	1	249.73	157.43	157.43	8.13	0.005	√
C_b	1	197.72	197.72	197.72	10.2	0.002	√
V×*I*	1	285.83	285.83	285.83	14.8	0.000	√
Error	112	2167.88	2167.88	19.36			
Total	19	3283.74					

d. ANOVA for depth

Source	DF	Seq SS	Adj SS	Adj MS	F	P	Sig.
V	1	0.00127	0.00009	0.00009	0.04	0.851	×
I	1	0.00473	0.00098	0.00098	0.40	0.526	×
T_{off}	1	0.03372	0.01388	0.01388	5.73	0.018	√
P	1	0.04508	0.04904	0.04904	20.25	0.000	√
N	1	0.17706	0.19650	0.19650	81.12	0.000	√
C_b	1	0.03608	0.03608	0.03608	14.89	0.000	√
V×*I*	1	0.00599	0.00599	0.00599	2.47	0.119	×
Error	112	0.27129	0.27129	0.00242			
Total	119	0.57522					

using a Nikon MM-400 microscope. Surface morphology of the cross section of machined surfaces was observed on a FEI Quanta-200 SEM.

3. RESULTS AND DISCUSSION

In order to understand the effect of input parameters on different response variables, statistical analysis using analysis of variance (ANOVA) has been performed (Table 2 *a-d*).

3.1 Analysis of material removal rate (MRR)

The MRR values in Table 1 show that the highest MRR (0.0417 mm^3/min) was achieved for 3rd experiment (1st replication) and the lowest MRR (0.0064 mm^3/min) was for 5th experiment. ANOVA for material removal rate (MRR) is presented in Table 2-*a*.

The ANOVA results show that discharge current (*I*) and rotational speed of the electrode (*N*) are the significant factors (at 95% confidence level) that influence the MRR (see Table 2-*a*). It is observed that interaction of *V*×*I* was not significant in influencing MRR. The trends of each factor in main effects plots are determined using analysis of means (AOM) plots presented in Fig. 2 *a-f*.

3.1.1 Effect of spindle speed (*N*) and current (*I*) on material removal rate (MRR)

The spindle speed (*N*) is statistically significant (at 95% confidence level) in influencing MRR (see Table 2-*a*). In addition, it appears from the main effects plot depicted in Fig. 2-*e* that there is an increase in MRR, when the spindle speed (*N*) increases 2.5 times. It was found that providing electrode rotation is always favorable during an EDM process, as the tool rotation generates whirl, to help flush debris out, which consequently improves the MRR.

Statistical analysis using ANOVA (see Table 2-*a*) reveals that discharge current (*I*) is the second significant parameter. The main effects plot (see Fig.2-*b*) indicates that MRR increases by 46%, with current (*I*). As current increases, electron density in plasma increases, causing an increase in MRR. However, helium is a light weight gas. As gap distance increases, relatively large expansion of plasma results in lower energy for machining. These effects cause a low MRR.

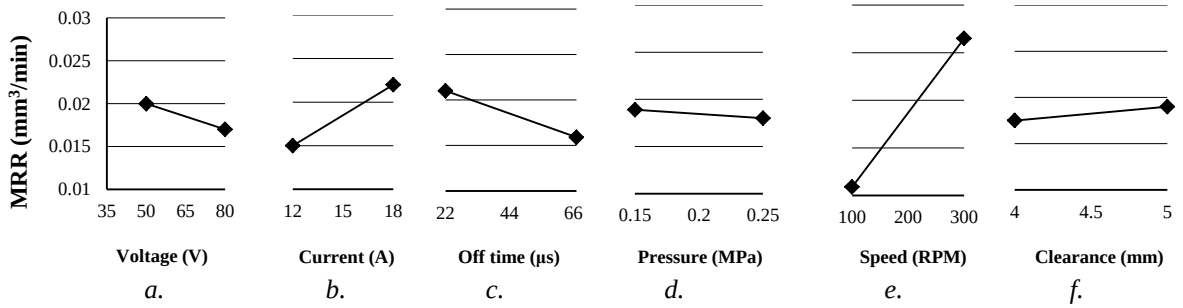

a. *b.* *c.* *d.* *e.* *f.*

Fig. 2 *a-f* Main effects plots of input parameters associated with MRR

3.1.2 Effect of other factors

Pulse off-time (T_{off}) is statistically significant at 90% confidence level in influencing MRR. With an increase in voltage, gap distance increases which leads to poor flushing efficiency [9].

3.1.3 Comparison with oxygen MRR data

In dry EDM using oxygen gas dielectric, ANOVA results showed that current (*I*), voltage (*V*) and speed of rotation (*N*) are the significant factors that influences MRR [10] (the highest and lowest levels of parameters used are same as used in the present study). The current (*I*) and speed of rotation (*N*) are the only significant factors in case of helium.

The variation of MRR with current and speed of rotation are the same for both oxygen and helium. However, highest value of MRR using oxygen reported in [10] was 0.811 mm^3/s which is far greater than helium (0.0417 mm^3/min) in the present study.

The trends of each factor in main effects plots are determined using analysis of means (AOM) plots in Fig. 3 *a-f*.

3..2 Analysis of tool wear rate (TWR)

The TWR values in Table 1 show that highest TWR (0.0449 mm^3/min) was observed for 8^{th} (1^{st} replication). ANOVA results for tool wear rate (TWR) is presented in Table 2-*b*. The ANOVA results show that there was no significant factor at 95% confidence level that affects TWR (see Table 2-*b*).

The pressure (*P*) appears to be significant at about 90% confidence level. With increases in pressure, TWR decreases as seen in Fig. 3-*d*. As pressure increases, more amount of helium gas has been present in the gap and thereby leads to high cooling, which results in less damage of tool electrode.

3.2.1 Comparison with oxygen TWR data

In dry EDM using oxygen gas dielectric, pressure (*P*) appeared to be significant at 90% confidence level in influencing TWR [10]. Therefore, the variation of TWR with pressure is the same for both oxygen and helium.

3.3 Analysis of oversize

Oversize in the hole dimension in comparison with the original electrode dimension has been estimated as OD error (outside diameter error %). The oversize values in Table 1 show that the highest oversize (-17.1%) was observed for 4^{th} experiment and the lowest oversize (0.33%) was for 6^{th} experiment. ANOVA for oversize have been presented in Table 2-*c*.

The ANOVA results show that, discharge current (*I*), rotational speed of the electrode (*N*), shield clearance at bottom (C_b) and interaction of $V \times I$ are the significant factors (at 95% confidence level) that influence the oversize (see Table 2-*c*). The trends of each factor are in analysis of means (AOM) plots in Fig. 4 *a-f*. Fig. 4-*g* presents the interaction plot of $V \times I$. With the increase in current (*I*) and speed (*N*), oversize increases and with the increases in shield clearance, oversize decreases as shown in the Fig. 4 *a-f*.

It is known that current (*I*) is directly proportional to MRR .and is more sensitive to the diameter as compared to depth of hole [9], therefore oversize increases with an increase in current. As speed of rotation (*N*) increases, possibly wobbling of tool electrode increases, which results in oversize. For low clearance of shield, less space has been available for debris removal, which possibly leads to arcing and results in oversize of the hole. It was evident from Fig. 4-*g*, that both lowest (50 V, 12 A) and the highest (80 V, 18 A) values of voltage and current gives lower oversize.

3.3.1 Comparison with oxygen oversize data

In dry EDM using oxygen gas dielectric, analysis of oversize for oxygen assisted dry EDM [10] was done at three locations, viz., entry, 50% depth and 90% depth of each hole machined. The ANOVA results showed that at entry of the hole, current and clearance of the shield at bottom are the significant parameters that govern the oversize. At 50% depth, current, oxygen pressure and spindle speed are significant. At 90% depth of hole, spindle speed was the only statistically significant parameter.

In the present study, discharge current, rotational speed of the electrode, shield clearance at bottom and interaction of $V \times I$ are the significant factors. However, the variation of oversize with current, speed of rotation and shield clearance are same for both oxygen and helium.

3.4 Analysis of depth of hole

The depth values presented in Table 1 show that the highest depth (0.38 mm) was achieved for 2^{nd} experiment (1^{st} replication) and the lowest depth (0.12 mm) were for 1^{st} and 8^{th} experiments (2^{nd} replication). ANOVA for depth values have been presented in Table 2-*d*.

The pulse-off time (T_{off}), Pressure (*P*), speed (*N*) and shield clearance at bottom (C_b) are significant in influencing depth of hole (see Table 2-*d*). With the increase of pulse-off time (T_{off}), depth decreases and with the increase of pressure (*P*),speed (*N*) and clearance (C_b), depth increases, as presented (see Figs. 5 *c*, *d* and *e*).

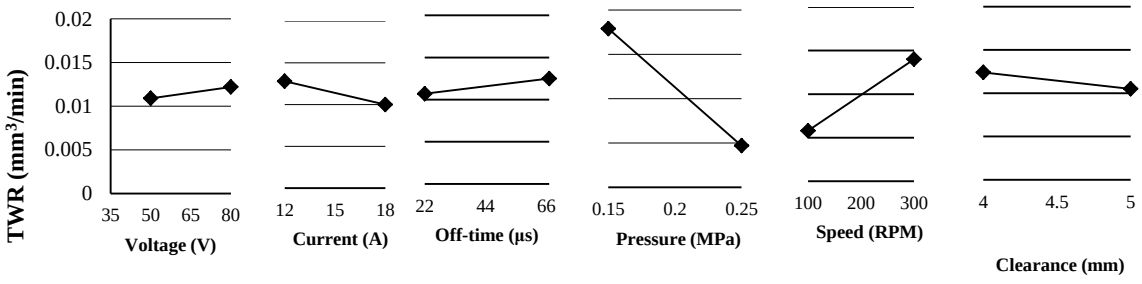

a. *b.* *c.* *d.* *e.* *f.*

Fig. 3 *a-f* Main effects plots of input parameters associated with TWR

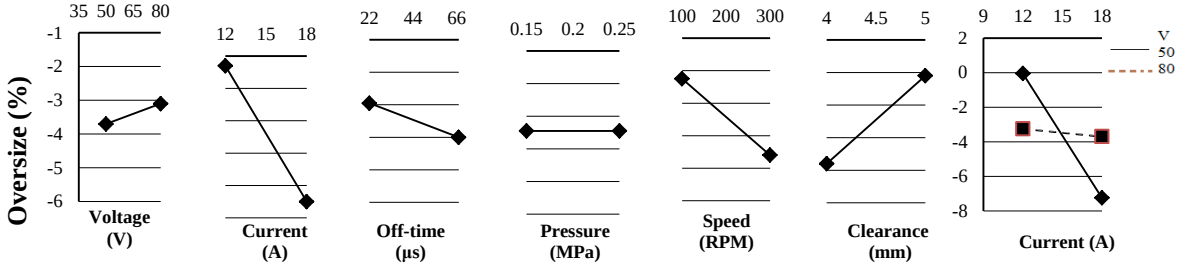

a. *b.* *c.* *d.* *e.* *f.* *g.*

Fig. 4 *a-g* Main effects plots of input parameters associated with oversize

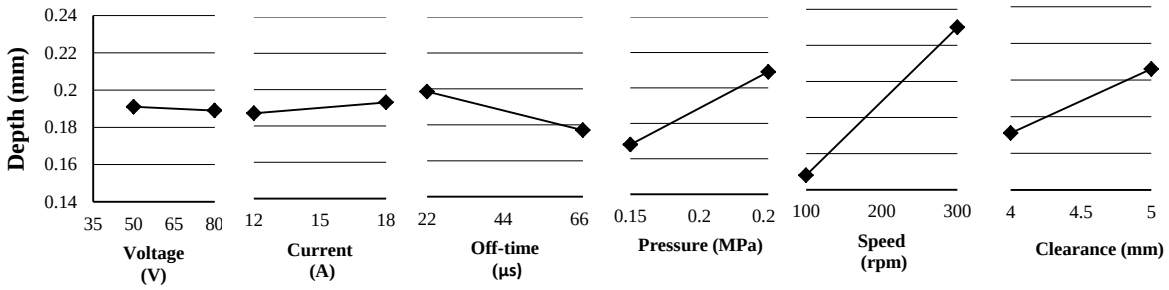

a. *b.* *c.* *d.* *e.* *f.*

Fig. 5 *a-f* Main effects plots of input parameters associated with depth achieved

All the dry EDM experiments were done at a constant pulse-on time (T_{on}) of 200 µs. Therefore, with an increase in pulse-off time (T_{off}), energy decreases, resulting in low depth. As the input pressure (P) increases, debris flushing increases, due to higher velocity of helium gas reaching the surface, which results in high value of depth. Similarly increase in the rotation speed (N) increases the depth.

3.5 Machined surface topography analysis

The analysis of surface topography was performed for dry EDM machined samples that correspond to the severest and the mildest conditions of MRR, TWR, oversize and depth at various magnifications (80X, 300X, 600X, 1200X, and 2400 X). A close examination of images showed that in few cases, micro-cracks have been developed due to thermal stresses.

Large spherical debris particles (globular solidifications) were formed because helium gas surrounds the molten material and cools the material. Few blow holes were formed due to entrapped helium gas. A few black patches indicate the presence of carbon element on the machined surfaces. The morphology of dry EDMed surfaces using helium gas is relatively far better than that using oxygen gas. Typical SEM micrographs of a cross-section of dry EDMed hole using oxygen and helium respectively are presented in Fig.6 *a-b*.

3.5.1 Comparison with topography of dry EDMed surfaces using oxygen gas

The dry EDMed surfaces using oxygen gas dielectric showed many large and deep micro-cracks were found due to high thermal loading [10]. However, in case of helium, very few micro-cracks were found because of sufficient

cooling action due to high heat capacity of helium gas dielectric.

The blow hole formation tendency was also found to be lesser in the present case, as compared to the dry EDM using oxygen gas. The river lines and dimples indicating stresses on dry EDMed surfaces were also not present in the case of dry EDM using helium gas, which was present in the case of dry EDM using oxygen gas dielectric.

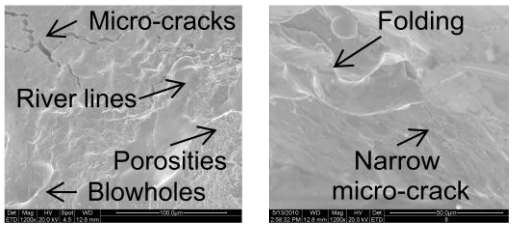

Fig.6 *a-b* A SEM micrograph of dry ED machined hole using *a.* oxygen and *b* helium gases (magnification: 1200X,), parametric conditions: (50 V, 18 A,33 µs,0.15 MPa, 100 RPM and 5 mm).

3.5.1 Comparison with topography of dry EDMed surfaces using oxygen gas

The dry EDMed surfaces using oxygen gas dielectric showed many large and deep micro-cracks were found due to high thermal loading [10]. However, in case of helium, very few micro-cracks were found because of sufficient cooling action due to high heat capacity of helium gas dielectric. The blow hole formation tendency was also found to be lesser in the present case, as compared to the dry EDM using oxygen gas. The river lines and dimples indicating stresses on dry EDMed surfaces were also not present in the case of dry EDM using helium gas, which was present in the case of dry EDM using oxygen gas dielectric.

4. Conclusions

The following conclusions are derived from the dry EDM investigation using helium gas dielectric:-

- In the dry EDM process using helium gas dielectric, the speed of rotation (*N*), current (*I*) and pulse off-time (T_{off}) control the MRR. On the contrary, in the dry EDM using oxygen gas dielectric, current (*I*), voltage (*V*) and speed of rotation (*N*) were the factors controlling the MRR.
- In case of dry EDM with helium gas, the pressure of pas (*P*) appears to be the controlling factor for TWR.
- In dry EDM using helium, current (*I*), spindle speed (*N*), shield clearance (C_b) and the interaction $V \times I$ are the controlling factors for OD oversize.
- The pulse-off time (T_{off}), pressure (*P*), speed of rotation (*N*) and shield clearance (C_b) influence statistically on the depth achieved in the process.
- Similarly, SEM micrographs of dry EDMed surfaces using helium gas dielectric showed a few micro-cracks and had a glowing appearance, which indicates that the quality of surfaces generated using helium is better as compared to oxygen.

Acknowledgement

The authors wish to acknowledge Department of Science and Technology, Government of India forproviding funding for this work. We also thank our collaborator, M/s Electronica Machine Tools, Pune for providing technical support to this work.

5. REFERENCES

[1] Ramani, V and Cassidenti (1985), Inert gas electrical discharge machining, NASA Technical Brief Number NPO 15660

[2] M. Kunieda, M. Yoshida, N. Taniguchi (1997), Electrical Discharge Machining in gas, Annals of the CIRP, Vol. 46(1), pp 143-146

[3] M. Kunieda, Y. Miyoshi, T. Takaya, N. Nakajima, Y. ZhanBo, M. Yoshida (2003), High Speed 3D Milling by Dry EDM, Annals of the CIRP, Vol. 52(1), pp 147-150

[4] Z. Yu, T. Jun, K. Masanori (2004), Dry electrical discharge machining of cemented carbide, Journal of Materials Processing Technology, Vol. 149, pp 353-357

[5] Q.H. Zhang, R. Du, J.H. Zhang, Q.B. Zhang (2006), An investigation of ultrasonic-assisted electrical discharge machining in gas, International Journal of Machine Tools & Manufacture, Vol. 46, pp 1582-1588

[6] C.C. Kao, J. Tao, A.J. Shih (2007), Near dry electrical discharge machining, International Journal of Machine Tools & Manufacture, Vol. 47, pp 2273-2281

[7] J. Tao, A.J. Shih, J. Ni (2008), Near-Dry EDM Milling of Mirror-Like Surface Finish, International Journal of Electrical Machining No. 13

[8] J. Tao, A.J. Shih, J. Ni (2008), Experimental Study of the Dry and Near-Dry Electrical Discharge Milling Processes, Journal of Manufacturing Science and Engineering, Vol. 130 / 011002-1, DOI: 10.1115/1.2784276

[9] Sourabh K. Saha, S.K. Choudhury (2009), Experimental investigation and empirical modeling of the dry electric discharge machining process, International Journal of Machine Tools & Manufacture, Vol. 49, pp 297-308.

[10] P. Govindan, Suhas S. Joshi (2010), Experimental characterization of material removal in dry electrical discharge drilling, International Journal of Machine Tools & Manufacture, Vol. 50, pp 431–443.